THE JOURNAL OF PHYSICAL CHEMISTRY A LETTERS

**2007,** *111,* 2458−2460
Published on Web 03/09/2007

# Direct Determination of Collision Rates beyond the Lennard-Jones Model through State-Resolved Measurements of Strong and Weak Collisions

**Daniel K. Havey,[†] Qingnan Liu,[†] Ziman Li,[†,‡] Michael Elioff,[‡] Maosen Fang,[‡] Joshua Neudel,[‡] and Amy S. Mullin*[,†,‡]**

*Department of Chemistry and Biochemistry, University of Maryland, College Park, Maryland 20742, and Department of Chemistry, Boston University, Boston, Massachusetts 02215*

*Received: February 13, 2007*

We describe a new approach for measuring absolute rates for molecular collisions including contributions of both strong and weak collisions. Elastic and inelastic collisions are monitored using high-resolution transient IR spectroscopy by measuring increases in the velocity distributions of individual rotational states of scattered molecules. Weak collisional energy transfer is detected by measuring velocity increases for the low-energy rotational states. This technique is illustrated for the collisional relaxation of highly vibrationally excited pyrazine (108 kcal/mol) with HOD. The observed collision rate is nearly twice the Lennard-Jones collision rate.

## Introduction

The lack of accurate collision rates for molecules is a long standing hindrance to a full understanding of energy transfer and unimolecular reactions.[1−3] Collisions that remove energy from highly vibrationally excited molecules compete directly with unimolecular decomposition. Quantifying the importance of a particular energy transfer pathway requires knowledge of the absolute rate of collisions. One challenge in measuring collision rates is that elastic and nearly elastic collisions scatter molecules with small changes in energy, making it difficult to determine experimentally whether or not a collision has occurred. Frequently used models for neutral collision partners rely on hard sphere (HS), Lennard-Jones (LJ), or Sutherland potentials.[4] The LJ and Sutherland potentials account for long range attraction, and collision rates based on these potentials are generally 2−3 times larger than those determined using a hard sphere potential. Collisions between an ion and a polarizable bath gas are routinely characterized using the Langevin collision rate that is typically 1 order of magnitude larger than LJ collision rates.[5] However, these models often yield molecular collision rates that differ substantially from rates observed in experiments and simulations.[6−13] Energy transfer probabilities based on calculated collision rates can lead to erroneous interpretations of quenching efficiencies. For example, polar molecules such as $H_2O$ are notorious for having unusually large average energy transfer $\langle\Delta E\rangle$ in collisions with highly vibrationally excited molecules.[13−15] A large $\langle\Delta E\rangle$ value could indicate that strong collisions govern the quenching process. However, state-resolved studies show that $H_2O$ gains relatively small amounts of rotational and translational energy following collisions with vibrationally excited molecules and that its enhanced quenching efficiency stems from large collision and energy transfer rates.[16,17] Having the means to get accurate collision rates would address this problem. Here we report new measurements that allow us for the first time to determine molecular collision rates by measuring directly the product state distributions and rates of appearance for the scattered molecules that result from both strong and weak collisions. These measurements include contributions from elastic and inelastic collisions that lead to changes in velocity and/or rotational quantum state. We illustrate this approach using data for collisions of highly vibrationally excited pyrazine ($E_{vib} = 108$ kcal/mol) with isotopically labeled water. We find that the observed collision rate is more than 70% larger than the LJ rate.

## Experimental Methods

Highly vibrationally excited pyrazine (Py) was generated with pulsed excitation at $\lambda = 266$ nm at a total pressure of 25 mTorr in a 3 m flowing gas collision cell. High-resolution transient IR absorption spectroscopy near $\lambda = 2.7$ $\mu$m was used to measure the time-dependent population changes in rotational states $J_{K_a,K_c}$ of HOD that result from single collisions with vibrationally excited pyrazine under isotropic conditions.

$$\mathrm{Py}(E_{vib}) + \mathrm{HOD} \xrightarrow{k_J} \mathrm{Py}(E_{vib} - \Delta E) + \mathrm{HOD}(000, J_{K_aK_c}, V_{el}) \quad (1)$$

IR absorption probes population changes for individual rotational states of HOD molecules in their ground vibrationless state (000). Nascent HOD populations resulting from single collisions with hot pyrazine were determined at $t = 1$ $\mu$s following the 266 nm pulse. The 1 $\mu$s probe time is well before the average collision time of 3 $\mu$s and the transient absorption signals are directly proportional to population changes due to collisions. The velocity distributions of the scattered molecules were obtained by measuring the nascent Doppler broadening of

* Corresponding author. E-mail address: mullin@umd.edu.
[†] University of Maryland.
[‡] Formerly at Boston University.

10.1021/jp0712497 CCC: $37.00 

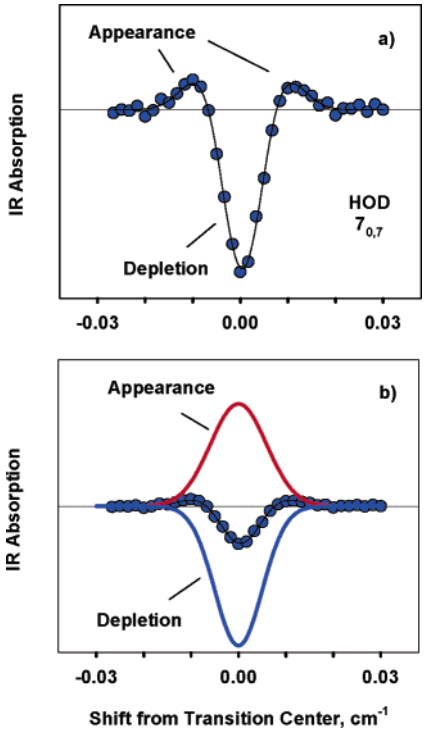


**Figure 1.** (a) Transient line profile for scattered HOD(000) molecules in the 707 rotational state following collisions with vibrationally excited pyrazine. Thermally populated HOD molecules are depleted via collisions at the center absorption frequency. Scattered molecules with increased velocities appear in the wings of the line profile. (b) Fitting to a double Gaussian function yields nascent appearance (red) and depletion (blue) populations.

individual IR transitions wherein transient HOD populations were measured at 1 $\mu$s as a function of IR wavelength. The transient line-profile measurements are necessary to account for all HOD molecules that scatter into an individual HOD rotational state. HOD molecules that are scattered into final states that are not populated at 300 K show only appearance signals. The line profiles for these states are Gaussian in shape as expected for an isotropic distribution of scattered molecules. HOD molecules that are scattered into final states that have ambient population prior to collisions with hot donor molecule are distinguished from the 300 K background in two ways. First, HOD molecules that are scattered into a final rotational state show a positive-going transient absorption signal due to appearance and the molecules that are scattered out of that state show a negative-going transient absorption signal due to population depletion. Second, the molecules that scatter into an HOD rotational state have broader Doppler profiles than the ambient background molecules that contribute to depletion. Thus, the transient line profiles for the low-J states of HOD are composed of two Gaussian profiles, one for appearance and one for depletion. Such a transient line profile is shown in Figure 1a for the HOD $7_{0,7}$ state.

## Results

The HOD $7_{0,7}$ state ($E_{rot}$ = 1.15 kcal/mol) is populated by thermal energy at 300 K prior to collisions with pyrazine and depletion of the initial population dominates the transient IR signal at line center. The appearance of scattered HOD molecules is evident in the wings of the line profile, where molecules with higher velocities are detected. For a given rotational state, the population of HOD molecules that appears following collisions with hot pyrazine is distinct from the initial

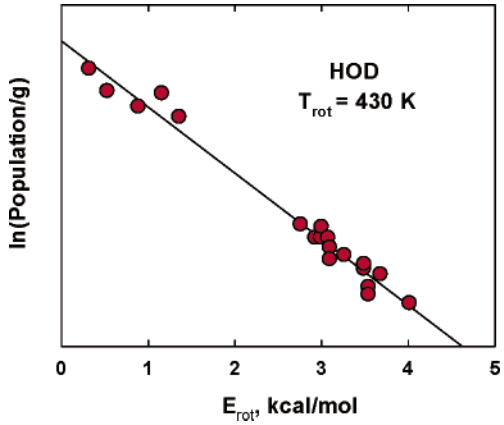


**Figure 2.** Nascent rotational energy distribution of HOD(000) following quenching collisions of vibrationally hot pyrazine. Energy transfer due to weak and strong collisions fits to a single rotational distribution.

thermal population that is depleted through collisions. These two components are separated by fitting the transient line profile to a double Gaussian, as shown in Figure 1b. The appearance curve in red corresponds to the velocity distribution for all HOD molecules scattered into the $7_{0,7}$ state and includes population from both elastic and inelastic collisions. Previous work has shown that the scattered molecules in these studies have an isotropic velocity distribution.[18] The Doppler profiles are 1-dimensional projections that provide a complete description of the full 3-dimensional distribution, thereby accounting for all HOD molecules that are scattered due to collisions with the activated donor. As the rotational energy of HOD increases, the initial state population decreases and transient signals show only appearance of scattered molecules. Our experiments indicate that the kinetic energy of the scattered HOD molecules in low- and high-energy rotational states is approximately twice the 300 K precollision value.

## Discussion

We have measured appearance populations for a number of HOD rotational states with energies between $E_{rot}$ = 0.3 and 4 kcal/mol. These data provide an excellent description of the distribution of rotational energy in HOD(000) molecules that have undergone single collisions with vibrationally hot pyrazine. Figure 2 is a semilog plot showing the population of a representative number of HOD rotational states as a function of the rotational energy. The nascent distribution of scattered HOD molecules is well described by a single rotational temperature of $T_{rot} = 430 \pm 50$ K. When only the high-energy states are fit, $T_{rot}$ is within 3% of this result. This result is important because it shows for the first time that weak collisions of a highly vibrationally excited molecule can be described by the same rotational distribution as the strong collisions. HOD states with midrange energies between 1.5 and 2.5 kcal/mol are not included in this analysis. For these states, the appearance and depletion signals are comparable and the resulting signal levels are near our current detection limit.

The inclusion of population data for the low-energy rotational states of HOD yields an excellent description of the scattered HOD molecules from which we determine the collision rate. For a discrete set of states indexed by J, the average energy for these states is the sum of the fractional population $f_J$ times the energy $E_J$ of each state. The populations of scattered HOD(000) molecules are shown in Figure 2 and have a rotational temperature $T_{rot}$. The average rotational energy of

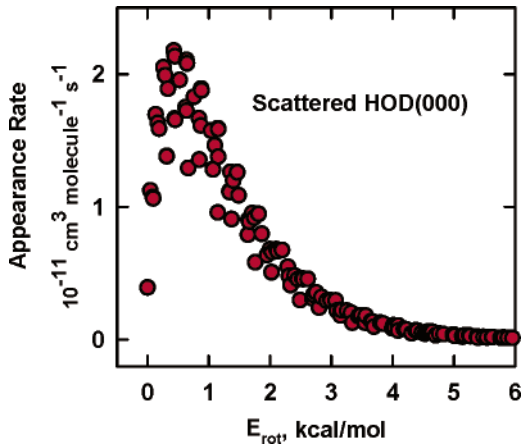


**Figure 3.** Energy transfer rate constants *kJ* for appearance of HOD-(000) from collisions with hot pyrazine.

the scattered HOD(000) molecules is

$$\langle E_{\mathrm{rot}}\rangle_{\mathrm{obs}} = \sum_{\mathrm{J}} f_{\mathrm{J}} E_{\mathrm{J}} = \sum_{\mathrm{J}} \frac{g_{\mathrm{J}} \mathrm{e}^{-E_{\mathrm{J}}/k_{\mathrm{B}}T_{\mathrm{rot}}}}{Q_{\mathrm{rot}}} E_{\mathrm{J}} = 1.25 \pm 0.16 \text{ kcal/mol} \quad (2)$$

Equivalently the fraction of scattered HOD molecules in each state is the appearance rate $k_{\mathrm{J}}$ divided by the collision rate, $f_{\mathrm{J}} = k_{\mathrm{J}}/k_{\mathrm{col}}$. We have measured rate constants for the appearance of a number of the HOD(000) states shown in Figure 2. These data are combined with the HOD rotational temperature to give rate constants for the appearance of the full distribution of scattered HOD(000) molecules, as shown in Figure 3. The LJ collision rate at 300 K for pyrazine−HOD collisions is $k_{\mathrm{LJ}} = 6.3 \times 10^{-10}$ cm$^3$ molecule$^{-1}$ s$^{-1}$. The LJ parameters $\sigma = 3.96$ Å and $\epsilon = 0.894$ kcal/mol for pyrazine/HOD collisions are based on established combining rules of $\sigma$ and $\epsilon$ parameters for the collision partners.[19] The well depth parameter $\epsilon$ contains the effect of attraction due to dipole−induced-dipole forces.[4] Using this approach, the average rotational energy of the scattered HOD molecules is 1.7 times larger than $\langle E_{\mathrm{rot}}\rangle_{\mathrm{obs}}$.

$$\langle E_{\mathrm{rot}}\rangle_{\mathrm{LJ}} = \sum_{\mathrm{J}} f_{\mathrm{J(LJ)}} E_{\mathrm{J}} = \sum_{\mathrm{J}} \frac{k_{\mathrm{J}}}{k_{\mathrm{LJ}}} E_{\mathrm{J}} = 2.11 \pm 0.53 \text{ kcal/mol} \quad (3)$$

The discrepancy in $\langle E_{\mathrm{rot}}\rangle$ values from eqs 2 and 3 stems directly from the choice of collision rate. Using a hard sphere collision rate $k_{\mathrm{HS}} = 3.2 \times 10^{-10}$ cm$^3$ molecule$^{-1}$ s$^{-1}$ leads to an even larger difference with $\langle E_{\mathrm{rot}}\rangle_{\mathrm{HS}} = 3.0\langle E_{\mathrm{rot}}\rangle_{\mathrm{obs}}$.

We can use these results to obtain a direct measurement of the collision rate. Using $\langle E_{\mathrm{rot}}\rangle_{\mathrm{obs}}$ from eq 2 as a constraint in eq 3 directly yields a collision rate of $k_{\mathrm{col}} = 1.07 \times 10^{-9}$ cm$^3$ molecule$^{-1}$ s$^{-1}$, which is 1.7 times larger than the LJ collision rate. Equivalently, the sum of $k_{\mathrm{J}}$ over all HOD J-states yields $k_{\mathrm{col}}$. This value of $k_{\mathrm{col}}$ includes all collisions that scatter HOD-(000) molecules and is a lower limit to the total collision rate because scattering of HOD molecules in the (000) state is just one possible outcome of collisions. Additional energy-transfer and reactive channels may also occur. Vibration-to-vibration (V−V) exchange could lead to excitation of HOD stretching and bending modes. However, previous studies of pyrazine relaxation by $H_2O$ show that vibration-to-rotation/translation (V−RT) energy transfer accounts for ∼96% of the energy transfer and that V−V exchange is relatively minor.[16,17] V−V transfer into the bend (1595 cm$^{-1}$) of $H_2O$ has a rate $k(010) = 4.4 \times 10^{-11}$ cm$^3$ molecule$^{-1}$ s$^{-1}$ that is 4% of the V-to-RT rate $k(000) = 1.08 \times 10^{-9}$ cm$^3$ molecule$^{-1}$ s$^{-1}$. No evidence has been seen for collisional excitation of water's stretching modes (3657 and 3755 cm$^{-1}$), which are of larger frequency than any single vibration in pyrazine. We expect that the HOD bend (1402 cm$^{-1}$) and OD stretch (2724 cm$^{-1}$) will be excited to some extent in collisions with vibrationally hot pyrazine but that the rates for these channels are likely to be small relative to the V−RT pathway.

A possible source of HOD is the isotope exchange reaction between $D_2O$ and vibrationally hot pyrazine. This reaction does not proceed at 300 K but could be promoted by the large internal energy of pyrazine. However, no evidence for HOD products from isotope exchange reactions was observed in our studies. We conclude that energy transfer is the sole outcome of collisions between vibrationally hot pyrazine and water. Because V−RT is the major relaxation pathway, the observed collision rate should be very close to the actual rate of collisions between vibrationally hot pyrazine and HOD.

This work shows that molecular collision rates can be determined directly from state-resolved energy gain data. To accomplish this, we have characterized the outcome of both strong and weak collisions to include the elastic or nearly elastic collisions that quench vibrationally excited molecules. The key is to account for all bath molecules that have undergone collisions with a vibrationally excited donor by measuring their state- and energy-resolved appearance. Weak collisions are measured from increases in the velocity spread of scattered molecules. For collisions of vibrationally excited pyrazine with HOD, we find that the observed collision rate is at least 1.7 times larger than the LJ collision rate. Whether the observed collision rate depends on the amount of vibrational energy in pyrazine remains to be determined from additional studies.

**Acknowledgment.** We thank Profs. Brooks Pate and W. Carl Lineberger for generously providing F-center laser equipment. The work at Boston University and University of Maryland was supported by the NSF (Grant Nos. 0316836 and 0552663, respectively). The Department of Energy provided additional equipment support (DE-FG02-06ER15761).

## References and Notes

(1) Chan, S. C.; Rabinovitch, B. S.; Bryant, J. T.; Spicer, L. D.; Fujimoto, T.; Lin, Y. N.; Pavlou, S. P. *J. Phys. Chem.* **1970**, *74*, 3160.
(2) Troe, J. *J. Chem. Phys.* **1977**, *66*, 4758.
(3) Snavely, D. L.; Zare, R. N.; Miller, J. A.; Chandler, D. W. *J. Phys. Chem.* **1986**, *90*, 3544.
(4) Hirschfelder, J. O.; Curtiss, C. F.; Bird, R. B. *Molecular Theory of Gases and Liquids*; John Wiley and Sons: New York, 1964.
(5) Su, T.; Bowers, M. T. *Gas Phase Ion Chem.* **1979**, *1*, 83.
(6) Hinchen, J. J.; Hobbs, R. H. *J. Chem. Phys.* **1976**, *65*, 2732.
(7) Mourits, F. M.; Rummens, F. H. A. *Can. J. Chem.* **1977**, *55*, 3007.
(8) Durant, J. L.; Kaufman, F. *Chem. Phys. Lett.* **1987**, *142*, 246.
(9) Lendvay, G.; Schatz, G. C. *J. Phys. Chem.* **1992**, *96*, 3752.
(10) Whetton, N. T.; Lawrance, W. D. *J. Phys. Chem.* **1992**, *96*, 3717.
(11) Xue, B.; Han, J.; Dai, H.-L. *Phys. Rev. Lett.* **2000**, *84*, 2606.
(12) Tasic, U. S.; Parmenter, C. S. *J. Phys. Chem. B* **2004**, *108*, 10325.
(13) Michael, J. V.; Su, M. C.; Sutherland, J. W.; Carroll, J. J.; Wagner, A. F. *J. Phys. Chem. A* **2002**, *106*, 5297.
(14) Hippler, H.; Troe, J. Recent direct studies of collisional energy transfer in vibrationally highly excited molecules in the ground electronic state. In *Bimolecular Collisions*; Baggott, J. E., Ashfold, M. N. R., Eds.; Royal Society of Chemistry: London, 1989.
(15) Yerram, M. L.; Brenner, J. D.; King, K. D.; Barker, J. R. *J. Phys. Chem.* **1990**, *94*, 6341.
(16) Fraelich, M.; Elioff, M. S.; Mullin, A. S. *J. Phys. Chem. A* **1998**, *102*, 9761.
(17) Elioff, M. S.; Sansom, R. L.; Mullin, A. S. *J. Phys. Chem. A* **2000**, *104*, 10304.
(18) Mullin, A. S.; Michaels, C. A.; Flynn, G. W. *J. Chem. Phys.* **1995**, *102*, 6032.
(19) Lim, K. F. *Quantum Chem. Program Exchange Bull.* **1994**, *14*, 3.